

Introduction and recovery of point defects in electron-irradiated Te- and Si-doped GaAs studied by positron lifetime spectroscopy

K. Saarinen, A. P. Seitsonen, and P. Hautojärvi

Laboratory of Physics, Helsinki University of Technology, 02150 Espoo, Finland

C. Corbel

Institut National des Sciences et Techniques Nucléaires, Centre d'Etudes Nucléaires de Saclay, 91191 Gif-sur-Yvette Cedex, France

(Received 30 March 1995)

Positron lifetime experiments have been performed to study the recovery of point defects in electron-irradiated n -type GaAs, which has been completely compensated in the irradiation. Irradiation temperature was 20 K and isochronal annealings were performed from 77 to 650 K. After all annealings below 450 K positrons detect irradiation-induced Ga vacancies and Ga antisite defects in a negative charge state. The main recovery stage of Ga is at 200–300 K. The Ga antisites anneal out at 500 K. Since the n -type conductivity reappears also after annealing at 500 K, we conclude that the negative Ga antisites have an important role in the compensation of n -type GaAs in the electron irradiation. Removal of compensation at 500 K reveals irradiation-induced As vacancies, which are converted from positive charge state to neutral or negative. The As vacancies introduced in the irradiation have similar ionization levels to those found in as-grown GaAs. The As vacancies recover at 550–650 K and their introduction rate is about 0.5 cm^{-1} after annealing at 550 K. The low value of the introduction rate may indicate that the recovery of the As vacancies starts already before 550 K.

I. INTRODUCTION

Electron irradiation is an important technique in studying basic properties of intrinsic point defects in semiconductor crystals.^{1,2} The impinging electrons with an energy of about 1 MeV have enough kinetic energy to displace single atoms. Simple intrinsic defects like vacancies and interstitials can thus be created homogeneously at large depths. Recent simulations also show that antisite defects can be created directly during electron irradiation.³ The concentration of these defects can be controlled by varying the electron-irradiation fluence. After irradiation the recovery of the intrinsic defects can be followed by isochronal annealings of the samples.

The electron irradiation of n -type GaAs increases the resistivity of the material and finally creates a total compensation of the n -type conductivity. After low-temperature irradiation the recovery of the electrical properties was studied already by Thommen (1970).⁴ Those experiments showed that the removal of the irradiation-induced defects responsible for the compensation takes place in three stages centered at about 235, 280, and 520 K. However, the nature of these defects is still under discussion, and the atomic processes leading to the recovery of them have not yet been identified.

Positrons in solids are trapped at vacancy defects, which can be experimentally observed as an increase in the positron lifetime. The positron technique thus yields defect-specific information on the vacancy-type defects.^{5,6} In addition, positron measurements can be used to study negative ion-type acceptors, since positrons are localized at the Rydberg states around the negative ions at low temperatures.⁷ In earlier experiments on electron-

irradiated undoped GaAs, two intrinsic defects have been identified, namely the Ga vacancy and the Ga antisite.^{8,9} The Ga vacancies recover at 200–300 K, whereas the Ga antisites are stable at least up to 450 K. Both V_{Ga} and Ga_{As} are in a negative charge state when the Fermi level is at midgap, indicating that they may play a crucial role in the compensation of the n -type material. In earlier positron experiments, indications of an annealing stage around 500 K, have also been obtained.^{10,11}

In this work we have performed positron lifetime experiments to study the defects introduced in the electron irradiation of n -type GaAs. The fluences are high enough so that the samples have been compensated during irradiation. We find that Ga vacancies and Ga antisites are formed similarly in n -type GaAs and in undoped GaAs. The Ga vacancies anneal mostly at 200–300 K, but the concentration of the Ga antisites is unchanged over this temperature range. The electrical compensation of the irradiated samples is removed at 500 K, and we show that this stage is related to the recovery of the Ga antisite defect. After the loss of compensation, positrons also detect As vacancies introduced in the electron irradiation. Their ionization levels are found to be the same as those of the As vacancies observed in the as-grown GaAs. The thermal recovery of the irradiation-induced V_{As} is detected in the annealing at 550–650 K.

The rest of the paper is organized as follows. The details of the positron experiments and the basic physics of positron trapping are explained in Sec. II. The positron results in as-grown n -type GaAs are given in Sec. III. The results in irradiated GaAs are presented, interpreted, and discussed in the three following sections according to increasing annealing temperature: 100–300 K in Sec. IV,

300–600 K in Sec. V, and 600–700 K in Sec. VI. The observations of this work are compared to earlier electrical, optical, and electron paramagnetic resonance results in Sec. VII. Finally Sec. VIII concludes the paper.

II. EXPERIMENTAL ARRANGEMENTS AND DATA ANALYSIS

A. Experimental details

Positron lifetime experiments were performed in as-grown *n*-type single-crystal GaAs samples and in five irradiated samples (Table I). The GaAs ([Te]= 1×10^{17} cm⁻³) and GaAs([Si]= 3×10^{17} cm⁻³) samples were obtained from Cambridge Instruments, and they were grown by the liquid-encapsulated Czochralski (LEC) method. The GaAs([Te]= 5×10^{18} cm⁻³) crystal was obtained from MCP Electronic Materials, and the GaAs([Si]= 2.3×10^{18} cm⁻³) sample from Radiotechnique (RTC). These two samples were grown by the horizontal Bridgman (HB) technique.

The electron irradiations were performed with 1.5-MeV electrons at 20 K with a Van der Graaf accelerator at the Laboratoire des Solides Irradiés (Ecole Polytechnique—Paris). GaAs([Te]= 1×10^{17} cm⁻³) crystals were irradiated to electron fluences of $\Phi = 1 \times 10^{17}$ e⁻ cm⁻² and $\Phi = 5 \times 10^{17}$ e⁻ cm⁻², and the GaAs([Si]= 3×10^{17} cm⁻³) sample to the fluence of $\Phi = 5 \times 10^{17}$ e⁻ cm⁻². The heavily doped samples GaAs([Te]= 5×10^{18} cm⁻³) and GaAs([Si]= 2.3×10^{18} cm⁻³) were irradiated to fluences of $\Phi = 1 \times 10^{18}$ and 5×10^{17} e⁻ cm⁻², respectively.

After low-temperature irradiations the samples were mounted at 77 K to a liquid-nitrogen cryostat for positron lifetime measurements as a function of isochronal annealing from 100 to 350 K. After annealing at 350 K the samples were moved to another liquid-nitrogen cryostat for positron experiments as a function of annealing from 300 to 700 K. The 30-min annealings were performed *in situ* in the positron measurement cryostat in a vacuum of 10^{-4} mbar. The possible loss of As from the surface during the heat treatment at 300–700 K plays no role in the conventional positron lifetime experiments, because the positrons are implanted into the bulk at the mean depth of 40 μm in GaAs. By positron experiments we also verified experimentally that there is no recovery in the as-grown samples at annealing temperatures of

TABLE I. The electron-irradiated *n*-type GaAs samples studied in this work. The irradiation was performed with 1.5-MeV electrons at 20 K. The carrier concentrations given in the table correspond to values measured at 300 K before the irradiation.

Dopant atom	Carrier concentration (cm ⁻³)	Irradiation fluence (e ⁻ cm ⁻²)
Te	1×10^{17}	1×10^{17}
Te	1×10^{17}	5×10^{17}
Si	3×10^{17}	5×10^{17}
Si	2.3×10^{18}	5×10^{17}
Te	5×10^{18}	1×10^{18}

300–700 K. This observation is in good agreement with our earlier results.¹²

Positron lifetimes were measured with a conventional spectrometer with a time resolution of 245 ps. Two identical samples were sandwiched with a 20-μ Ci²²Na positron source deposited on a 1.5-μm Al foil. Typically 2×10^6 annihilation events were collected in each positron lifetime spectrum. After subtracting the background and the annihilations in the source materials (215 ps, 5.4%; 450 ps, 1.6%; and 1500 ps, 0.03%), the lifetime spectra were analyzed with one or two exponential components,

$$n(t) = n_0 [I_1 \exp(-\lambda_1 t) + I_2 \exp(-\lambda_2 t)], \quad (1)$$

convoluted with the Gaussian resolution function of the spectrometer. In Eq. (1), n_0 is the total number of collected annihilation events, the annihilation rate λ_i is the inverse of the positron lifetime ($\lambda_i = \tau_i^{-1}$), and I_i is the relative intensity of the lifetime component τ_i in the spectrum. The average positron lifetime is calculated as $\tau_{av} = \sum I_i \tau_i$. This parameter is insensitive to the decomposition procedure and even as small a change as 1 ps in its value can be reliably measured.

B. Data analysis with positron trapping models

In perfect semiconductors positrons are delocalized, and annihilate with a single lifetime τ_b . In the presence of defects, positrons as positive particles are able to be trapped at vacancies where the positron-ion repulsion is locally reduced. As a result of the trapping, positrons at vacancies annihilate from a localized state with the lifetime τ_v . Because the electron density in a vacancy is lower than in the bulk, the lifetime τ_v is always longer than the bulk lifetime τ_b . The positron trapping rate κ_v at the vacancies is the product of the vacancy concentration c_v and the positron trapping coefficient μ_v :

$$\kappa_v = \mu_v c_v. \quad (2)$$

The positron trapping coefficient μ_v depends strongly on the charge of the vacancy defect. The Coulomb repulsion between a positive vacancy and the positron prevents the positron trapping, and the trapping coefficient is practically zero.¹³ At neutral vacancies the trapping coefficient is typically $\mu_v = 1 \times 10^{15}$ s⁻¹, and its value is constant as a function of temperature.¹⁴ Positron trapping at negative vacancies may take place either directly or through a Rydberg precursor state, which leads to a temperature-dependent trapping coefficient.^{13,15} Experimental information on the temperature dependence of μ_v at negative vacancies in semiconductors has been recently obtained.^{15,16} In the case of negative Ga vacancies in GaAs, we have estimated that $\mu_v = 1.4 \times 10^{15}$ s⁻¹ at 300 K, and it increases by a factor of 9 when the temperature is lowered to 30 K.^{9,16}

When only one type of vacancy defect exists in a single charge state, the measured positron average lifetime is the superposition

$$\tau_{av} = (1 - \eta_v) \tau_b + \eta_v \tau_v, \quad (3)$$

where η_v is the fraction of positrons annihilating at the vacancies. Furthermore, the experimental second lifetime component τ_2 is equal to the lifetime at the vacancy: $\tau_2 = \tau_v$. The positron trapping rate at the vacancy can then be calculated as

$$\kappa_v = \frac{1}{\tau_b} \frac{\tau_{av} - \tau_b}{\tau_v - \tau_{av}} \quad (4)$$

Information on the vacancy concentration can thus be obtained by calculating the positron trapping rate κ_v , and absolute concentrations can be estimated if the trapping coefficient μ_v is known [see Eq. (2)].

At low temperatures the positron may be captured at Rydberg states of negative ion-type defects. These positron traps are shallow in the sense that the positron binding energy is so small (< 0.1 eV) that at high temperatures positrons are able to escape from ions to the delocalized state in the bulk. When both vacancies and negative ions exist in the material, the positron average lifetime is the superposition

$$\tau_{av} = (1 - \eta_{st} - \eta_v)\tau_b + \eta_{st}\tau_{st} + \eta_v\tau_v, \quad (5)$$

where η_{st} and η_v are the fractions of positrons annihilating at the ions and vacancies, respectively. The positron lifetime τ_{st} at the Rydberg state of the ions is very close to that of free positrons in the bulk: $\tau_{st} \approx \tau_b$. The trapping rate κ_{st} at the negative ions gives information on the concentration c_{st} of them through $\kappa_{st} = \mu_{st}c_{st}$, where μ_{st} is the positron trapping coefficient. At low temperatures when the positron is unable to escape thermally from the ions, the trapping rate κ_{st} can be calculated from the average lifetime as

$$\kappa_{st} = \frac{\kappa_v(\tau_v - \tau_{av}) + \lambda_b(\tau_b - \tau_{av})}{\tau_{av} - \tau_{st}}, \quad (6)$$

if the positron trapping rate at the vacancies κ_v is known. At higher temperatures positrons are able to escape from the Rydberg states of the ions, and the detrapping rate δ thus becomes comparable to the trapping rate κ_{st} . The detrapping rate can be written as

$$\delta = \mu_{st} \left[\frac{2\pi m^* k_B T}{h^2} \right]^{3/2} \exp \left[-\frac{E_{b,st}}{k_B T} \right], \quad (7)$$

where m^* is the effective mass of the positron and $E_{b,st}$ is the positron binding energy at the Rydberg state of the negative ion. Expressing the annihilation fractions η_{st} and η_v as functions of the trapping and detrapping rates, the positron average lifetime can be modeled. In the case of a single type of vacancy and shallow trap, we obtain

$$\begin{aligned} \eta_b &= 1 - \eta_{st} - \eta_v, \\ \eta_{st} &= \frac{\kappa_{st}}{\left[1 + \frac{\delta}{\lambda_{st}} \right] \left[\lambda_b + \kappa_v + \frac{\lambda_{st}}{\lambda_{st} + \delta} \kappa_{st} \right]}, \\ \eta_v &= \frac{\kappa_v}{\lambda_b + \kappa_v + \frac{\lambda_{st}}{\lambda_{st} + \delta} \kappa_{st}}. \end{aligned} \quad (8)$$

Equations (5)–(8) can be fitted to the temperature dependence of the experimental average lifetime, and the positron trapping coefficient μ_{st} and binding energy $E_{b,st}$ can be determined as fitting parameters. This analysis method yields values for μ_{st} and κ_{st} independently of each other [Eqs. (6) and (7)], which also means that the concentration of negative ions c_{st} can be determined.

In the analysis of the present data we have modeled the temperature dependence of the positron trapping coefficient at vacancies similarly as in the earlier works.^{15–17} The positron trapping coefficient at negative ions was assumed to vary as $T^{-0.5}$ with temperature, which is the result predicted by the theory.¹³ This type of analysis of the data has been explained in more detail earlier.⁹

III. POSITRON LIFETIMES IN AS-GROWN *n*-TYPE GaAs

Before the electron irradiation the samples were measured as a function of temperature from 80 to 550 K. The results in GaAs([Te] = 1×10^{17} cm⁻³) are shown in Fig. 1. The average lifetime first increases at 80–200 K and then decreases from 242 ps at 200 K to about 235 ps at 500 K. The temperature dependence of the average lifetime is completely reversible. At all temperatures the average lifetime is above the bulk lifetime (231 ps at 300 K).^{12,18} The lifetime spectrum could be decomposed into two components at temperatures above 150 K. As seen in Fig. 1, the second lifetime component τ_2 shows a transient behavior increasing from about 260 ps at 150 K to

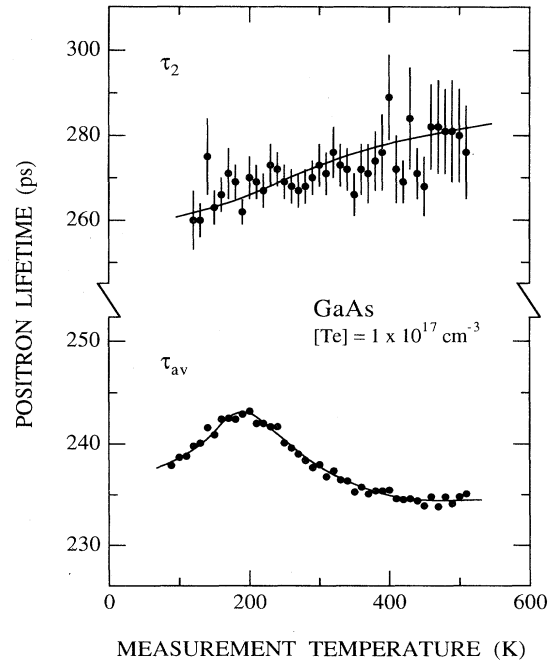


FIG. 1. Positron average lifetime and the second lifetime component as a function of measurement temperature in as-grown Te-doped GaAs with a carrier concentration of 1×10^{17} cm⁻³ at 300 K.

roughly 280 ps at 500 K. However, the intensity I_2 of this component decreases over the whole transient region from 70% to 30%. The lifetime τ_1 increases from 180 to 220 ps in the temperature range 150–550 K, and its value is roughly in agreement with the prediction of the simple trapping model.⁵

The temperature dependence of the positron lifetimes in as-grown n -type GaAs has been discussed in detail in our earlier publications.^{12,18} Since the positron average lifetime is greater than the bulk lifetime, native vacancy defects are observed in the as-grown GaAs(Te) sample of Fig. 1. Vacancy defects are commonly detected in the positron experiments in as-grown n -type GaAs. It has been shown that these defects exhibit two positron lifetime transitions as a function of the measurement temperature, and that the transitions are controlled by the position of the Fermi level in the energy gap.^{18,12} In the first transition the lifetime τ_2 of the positrons trapped at vacancies increases from 257 to 295 ps, and the transition takes place when the Fermi level is 30 meV below the conduction band. The lifetimes of 257 and 295 ps can be attributed to two well-defined positron annihilation states, and experimental values of τ_2 between these two lifetimes are superpositions of positron annihilations in the states corresponding to 257 and 295 ps, respectively. In the second transition the positron trapping at the vacancy defect with the lifetime 295 ps is gradually lost. This transition takes place when the Fermi level is 140 meV below the conduction band.

The Fermi-level-controlled positron lifetime transitions in as-grown n -type GaAs have been explained in terms of the ionization of the native As vacancy. The two different positron lifetimes of 257 and 295 ps correspond to negative and neutral charge states of the As vacancy. The As vacancy is ionized from negative to neutral when the Fermi level crosses an ionization level E_i of V_{As} at 30 meV below the minimum of the conduction band E_c . Similarly, the As vacancy is ionized to a positive charge state at $E_i = E_c - 140$ meV. In this transition, positron trapping at V_{As} disappears because the positive vacancy is repulsive to positrons. Positron lifetimes of 257 ps at V_{As}^- , 295 ps at V_{As}^0 , and 231 ps for the GaAs bulk are in good agreement with the theoretical calculations.^{19–21}

The experimental results of Fig. 1 are in perfect agreement with our earlier findings.^{12,18} The Fermi level in GaAs([Te] = 1×10^{17} cm⁻³) is at $E_c - 40$ meV at 300 K. It is thus expected that in this type of sample the ionization of the As vacancy from the negative (257 ps) to neutral (295 ps) charge state takes place at around room temperature. In Fig. 1 the transition is in fact observed as an increase in the second lifetime component τ_2 . The transition is wide: it starts at 100 K and continues up to above 500 K. However, the width is in good agreement with the Fermi function describing the populations of V_{As}^0 and V_{As}^- .¹⁸

The average positron lifetime in Fig. 1 decreases as a function of temperature at $T > 200$ K. This decrease reflects the ionization of the As vacancy from negative to neutral charge state as explained above. Although the second lifetime component τ_2 increases in this ionization from 257 to 295 ps, a decrease is detected in the average

lifetime. This is due to the smaller positron trapping coefficient at the neutral charge state of the As vacancy compared to that at the negatively charged V_{As} . At the highest measurement temperatures of 400–550 K the ionization of the As vacancy to a positive charge state also plays a role as the Fermi level approaches the ionization level at $E_c - 140$ meV. This transition also decreases the average lifetime, because positron trapping at the As vacancy is gradually lost.

However, the decrease of the average lifetime below 200 K cannot be explained by the ionizations of the native vacancies nor by the temperature dependence of the positron trapping coefficient. As explained in Sec. II, positrons may be captured at the Rydberg states of negative ions at low temperatures. The positron lifetime at the Rydberg state is close to that of free positrons in the bulk. If both negative ions and vacancies are present in the material, there is competition in the positron trapping at these defects at low temperatures. This effect yields to a decrease in the average lifetime, because fewer positron annihilations take place at vacancies. At high temperatures the influence of the negative ions is lost due to positron detrapping from them.^{7,9}

In as-grown n -type GaAs the negative ions may be residual impurities or native intrinsic point defects like antisites or interstitials.⁷ Their concentrations can be estimated by calculating the positron trapping rates κ_v and κ_{st} at the vacancies and ions using Eqs. (4) and (6), or by modeling the temperature dependence of the average lifetime as explained in Sec. II B. However, the positron trapping model of Sec. II B has to be generalized to include both negative and neutral charge states of the As vacancies.¹⁸ We further describe the ionizations of the As vacancies with the Fermi functions

$$[V_{As}^-]/[V_{As}] = \left\{ 1 + g_1^{-1} \exp \left[\frac{E_1 - E_F}{k_B T} \right] + g_1^{-1} g_2^{-1} \exp \left[\frac{E_1 + E_2 - 2E_F}{k_B T} \right] \right\}^{-1}, \quad (9)$$

$$[V_{As}^0]/[V_{As}] = \left\{ 1 + g_2^{-1} \exp \left[\frac{E_2 - E_F}{k_B T} \right] + g_1 \exp \left[-\frac{E_1 - E_F}{k_B T} \right] \right\}^{-1}, \quad (10)$$

where $g_1 = Z(V_{As}^-)/Z(V_{As}^0)$ and $g_2 = Z(V_{As}^0)/Z(V_{As}^+)$ are the ratios of the internal degeneracies $Z(V_{As})$ of the various charge states of the As vacancies. E_1 and E_2 are the $-/0$ and $0/+$ ionization levels of V_{As} , and E_F is the Fermi level. The fit was performed by weighting the positron trapping rates at negative and neutral V_{As} with Eqs. (9) and (10). The parameters E_1 , E_2 , g_1 , and g_2 were determined as fitting parameters, and similar results as earlier were obtained: $E_1 \approx E_c - 50$ meV, $E_2 \approx E_c - 100$ meV, $g_1 \approx 0.5$, and $g_2 \approx 0.25$.¹⁸ The inaccuracy of these values is roughly 30%. It originates mainly from the temperature dependence of the Fermi level, which was not measured but calculated simply by assuming that all

conduction electrons are emitted from a single donor level of the Te atoms.¹⁸ The fit further yields an estimate for the ratio of the positron trapping coefficients at negative and neutral states of the As vacancy: $\mu(V_{As}^-)/\mu(V_{As}^0) = 6 \pm 2$ at 300 K. With this ratio the positron trapping rate at V_{As}^- [denoted by $\kappa(V_{As}^-)$] and at the negative ions can be determined in the analysis, and these parameters were found to be insensitive to the exact temperature dependence of the Fermi level. The fitted function is shown by the solid line in Fig. 1.

In the data of Fig. 1 we obtain the trapping rates $\kappa_{st} = 36 \pm 1 \text{ ns}^{-1}$ and $\kappa(V_{As}^-) = 18 \pm 1 \text{ ns}^{-1}$ at 80 K. The fitted values for the positron binding energy and the trapping coefficient at negative ions were $E_{b,st} = 45 \pm 7 \text{ meV}$ and $\mu_{st} = (5 \pm 2) \times 10^{16} (\text{T/K})^{-0.5} \text{ s}^{-1}$. These values are close to those we obtained previously in electron-irradiated or as-grown GaAs.^{7,9,17} The concentration of negative ions in the as-grown reference sample is thus $c_{st} = (3 \pm 1) \times 10^{17} \text{ cm}^{-3}$. Using $\mu_v = 1.4 \times 10^{15} \text{ s}^{-1}$ for negative As vacancies at 300 K,⁹ we can estimate that the total concentration of As vacancies is $[V_{As}] = (1.1 \pm 0.2) \times 10^{17} \text{ cm}^{-3}$. The concentrations of vacancies and negative ions are thus of the same order of magnitude, roughly 10^{17} cm^{-3} .

Notice that the errors given above for κ_{st} , κ_v , $E_{b,st}$, and μ_{st} are calculated after fixing the parameters describing the ionization levels (E_1 , E_2 , g_1 , and g_2) and the ratio $\mu(V_{As}^-)/\mu(V_{As}^0)$ to their optimal values. This procedure is justified in cases where the same defects are found in different samples, and the main interest is in comparing the concentrations of vacancies and negative ions. In this work this is exactly our primary goal, since we study the changes in the defect concentrations as a function of the irradiation fluence and thermal annealing.

We conclude that in as-grown *n*-type GaAs native As vacancies are detected by positron experiments. These vacancies exhibit similar Fermi-level-controlled transitions which we observed earlier and attributed to thermal ionizations of the As vacancy.^{18,12} In addition to native vacancies, negative ion-type defects are also seen. The concentrations of both ions and vacancies are of the order of 10^{17} cm^{-3} , and both types of defects are stable in the annealing of samples at 600 K.

IV. RECOVERY OF IRRADIATION-INDUCED DEFECTS AT 100–300 K

A. Carrier compensation and native vacancies in electron-irradiated GaAs

Electron irradiation may create intrinsic vacancies, antisites, and interstitials as primary defects. These defects may be charged, and they can thus act as deep or shallow donors or acceptors. In the electron irradiation of GaAs it has been found that the *n*-type conductivity is very effectively compensated by the creation of acceptor defects.^{1,22} The introduction rate of acceptors has been estimated to be as high as $\Sigma_{acc} = 5 \text{ cm}^{-1}$ in 1-MeV electron irradiation at 300 K,^{23,24} and after 1.5-MeV irradiation the removal rate of carriers is about two times larger than after 1.0-MeV irradiation.¹ For example, we have ob-

served previously that *n*-type GaAs crystals with a carrier concentration of $n = 10^{16} \text{ cm}^{-3}$ are fully converted semi-insulating after 1.5-MeV room-temperature electron irradiation at a fluence of $\Phi = 10^{16} \text{ e}^- \text{ cm}^{-2}$.⁸ All our irradiated samples in the 10^{17}-cm^{-3} doping range have thus been totally compensated (Table I). The compensation is also probably very effective in samples doped to the range of $n = 10^{18} \text{ cm}^{-3}$, because the total number of acceptors produced is always larger than the concentration of *n*-type carriers, i.e., $\Sigma_{acc}\Phi > n$. After irradiation at 20 K the Fermi level is thus located at the midgap, at least up to the annealing temperature of 300 K. The compensation probably also remains to higher temperatures, because only 20–50% of the carrier removal recovers at 200–300 K.^{1,4,22}

In previous positron experiments on electron-irradiated *n*-type GaAs, the compensation of the material has been clearly seen.⁸ As explained in Sec. III, positrons reveal native As vacancies in as-grown *n*-type GaAs. In electron-irradiated samples, positron trapping at the native As vacancies is lost, since they become positively charged when the Fermi level moves toward the midgap.⁸ Because the compensation is very effective in the present samples, the native As vacancies are positive and not visible to positrons after electron irradiation. Thus the vacancy signal observed in the irradiated samples can be attributed to irradiation-induced vacancies.

On the other hand, positron experiments have been used to identify two intrinsic acceptors, which take part in the above-mentioned compensation mechanism. In semi-insulating (SI) GaAs, irradiation-induced Ga vacancies are detected.^{8,25} They are in a negative charge state and recover mainly at 200–300 K. The previous positron experiments also give direct evidence that negative ion-type defects are created in the electron irradiation.⁹ These defects act as shallow positron traps, and are stable at least up to 450 K. On the basis of the charge states predicted by theoretical calculations, the negative ions have been identified as Ga antisite defects.

B. Annealing effects in *n*-type GaAs compensated by electron irradiation

Figure 2 shows the positron average lifetime as a function of the isochronal annealing temperature in Te- and Si-doped GaAs. The samples were irradiated with 1.5-MeV electrons at 20 K, and the data in Fig. 2 were measured at 80 K. In all samples the average lifetime decreases at 200–300 K, indicating that the concentration of the irradiation-induced vacancies decreases at these annealing temperatures. This annealing stage is the same as that we previously attributed to the recovery of irradiation-induced vacancies in semi-insulating GaAs and in compensated *n*-type material.⁸ The defects can be identified as Ga vacancies, since they are negative when the Fermi level is at midgap. Irradiation-induced As vacancies are not detected in positron experiments, because their charge state is positive in semi-insulating and in fully compensated *n*-type GaAs.⁸ In the present data the decompositions of the lifetime spectra yield the second component of $\tau_2 = 260 \text{ ps}$ after annealing at $T \leq 300 \text{ K}$,

which is the same as that obtained for V_{Ga} in earlier experiments^{8,9} and theoretical calculations.^{19,20} The positron experiments of this work thus reveal Ga vacancies in electron-irradiated Si- and Te-doped GaAs. The recovery of V_{Ga} in the doped material is qualitatively similar to that observed earlier in SI GaAs.

However, the data in Fig. 2 are quantitatively very different from those obtained in semi-insulating GaAs. The level of the positron average lifetime before annealing is about 240 ps even after the largest irradiation fluence of $\Phi = 10^{18} \text{ e}^- \text{ cm}^{-2}$. This value is much smaller than the positron lifetimes detected in irradiated SI GaAs.^{8,9} For example, after $\Phi = 5 \times 10^{17} \text{ e}^- \text{ cm}^{-2}$ electron irradiation (1.5 MeV) of SI GaAs at 20 K, the average lifetime at 100 K is about 255 ps after annealing at 100 K.⁸ This quantitative difference indicates that either (i) far fewer Ga vacancies are created in Te- and Si-doped GaAs than in undoped SI GaAs in the electron irradiation, or (ii) the concentration of negative ions is much

larger in irradiated Te- and Si-doped material than in undoped GaAs. We shall show next that point (ii) is the right explanation for the difference.

C. Vacancies and negative ions after electron irradiation

Figure 3 shows the positron average lifetime as a function of measurement temperature in the $\Phi = 10^{17} \text{ e}^- \text{ cm}^{-2}$ electron-irradiated GaAs ($[\text{Te}] = 10^{17} \text{ cm}^{-3}$) sample. The temperature dependence has been measured after annealing the samples at temperatures of 150–450 K, as indicated in the figure. Results of a similar experiment in the $\Phi = 5 \times 10^{17} \text{ e}^- \text{ cm}^{-2}$ electron-irradiated GaAs ($[\text{Te}] = 10^{17} \text{ cm}^{-3}$) sample are presented in Fig. 4. Notice that the annealing curves of Fig. 2 can be obtained from the 80-K data points of Figs. 3 and 4.

As explained in Secs. II and III, the positron lifetime experiments as a function of the measurement temperature give information on the negative ions acting as shall-

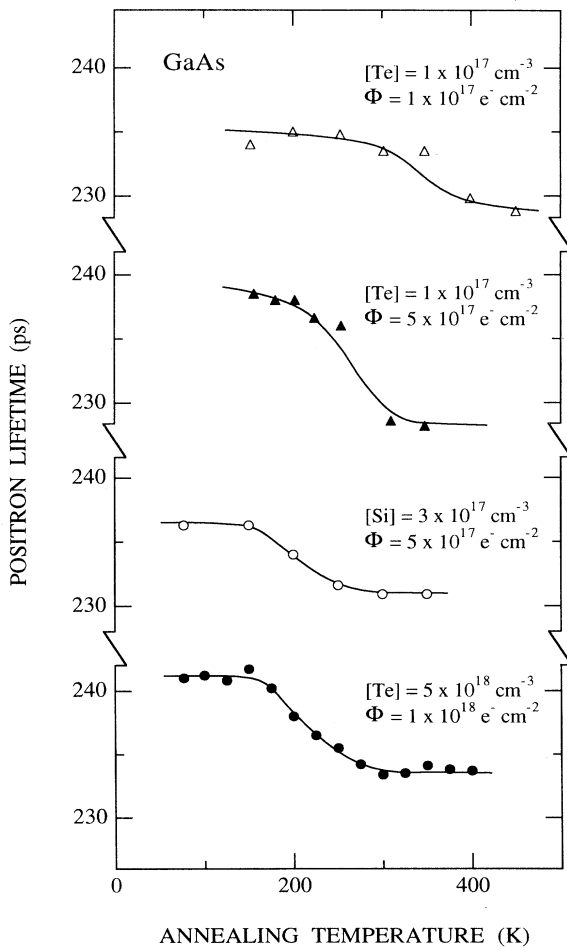


FIG. 2. Positron average lifetime as a function of the isochronal annealing temperature in electron-irradiated n -type GaAs. The measurement temperature is 80 K. The donor atom, the carrier concentration of the samples at 300 K before irradiation, and the irradiation fluence are indicated in the figure.

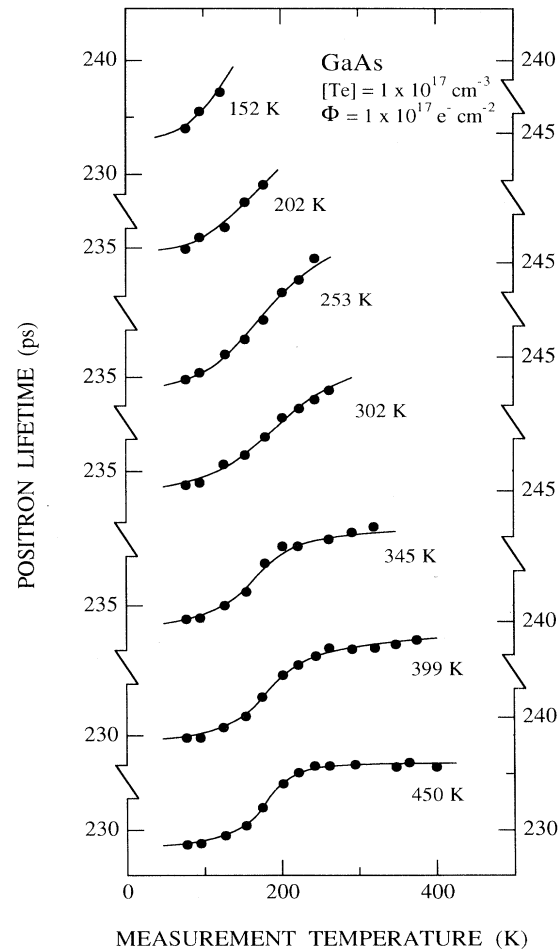


FIG. 3. Positron average lifetime as a function of the measurement temperature after annealing at the temperatures shown in the figure. The Te-doped GaAs sample has been electron irradiated to a fluence of $\Phi = 1 \times 10^{17} \text{ cm}^{-2}$. The carrier concentration of the sample was $1 \times 10^{17} \text{ cm}^{-3}$ at 300 K before irradiation.

low positron traps at low temperature. After all annealings at 150–450 K the positron average lifetime in Figs. 3 and 4 increases as a function of the measurement temperature. This increase is due to the detrapping of positrons from the negative ions, resulting in a larger fraction of annihilations at the vacancies (i.e., an increase in τ_{av}). At low temperatures the average lifetime in Figs. 3 and 4 becomes constant because the thermal energy of the positron is insufficient to facilitate the detrapping from the vacancies. At high temperatures of $T > 250$ K the positron lifetime in Fig. 3 again reaches a plateau. This behavior indicates that detrapping from the ions is complete, and only the vacancy defects are seen.

The analysis of positron detrapping indicates that if the positron binding energy at the negative ions remains the same, the increase of τ_{av} starts at about the same measurement temperature independently on the concentrations of the ions and vacancies.⁹ This takes place at about 100 K in all curves in Figs. 3 and 4, thus indicating

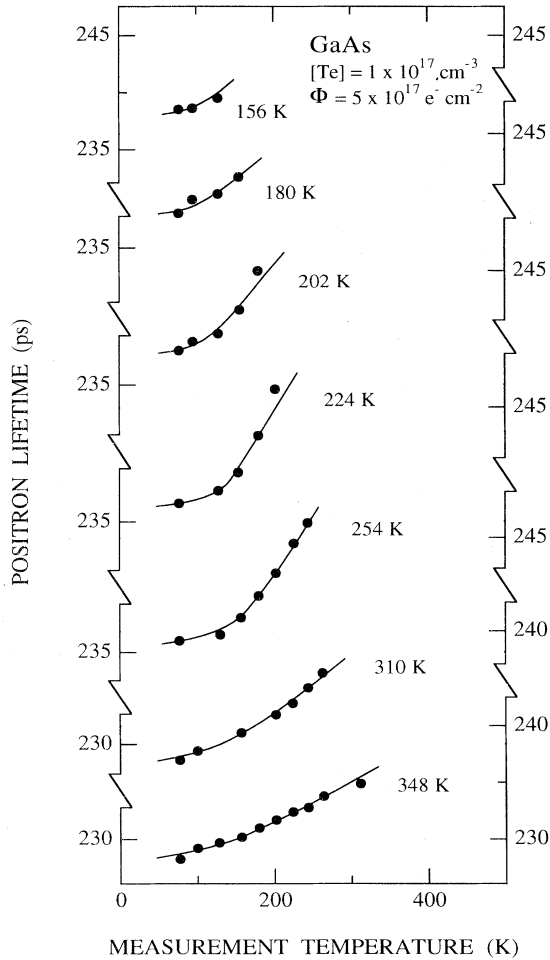


FIG. 4. Positron average lifetime as a function of the measurement temperature after annealing at the temperatures shown in the figure. The Te-doped GaAs sample has been electron irradiated to a fluence of $\Phi = 5 \times 10^{17} \text{ cm}^{-2}$. The carrier concentration of the sample was $1 \times 10^{17} \text{ cm}^{-3}$ at 300 K before irradiation.

that the positron binding energy is in all cases the same, about 50 meV.⁹ However, there are marked differences between the data shown in Figs. 3 and 4. First, the values of the average lifetime are different. After annealing at temperatures below 250 K, τ_{av} in the curves of Fig. 4 is generally higher than in the curves of Fig. 3, but after annealing at higher temperatures the order is the reverse. Second, there is a clear plateau at high measurement temperatures in the data of Fig. 3, but this plateau is completely missing in Fig. 4.

The quantitative analysis using positron trapping models reveals two distinct features in the τ_{av} vs T curve, when the concentration of negative ions increases.⁹ First, the average lifetime decreases in the low-temperature region of the curve, and second, a larger temperature is needed to reach the high-temperature plateau of the τ_{av} vs T curve. The latter is exactly the difference between the sets of curves in Figs. 3 and 4: when the electron-irradiation fluence is larger (Fig. 4), no plateau of the average positron lifetime is detected at high temperatures. This behavior indicates that the concentration of the negative ions is much larger in the GaAs(Te) sample which is irradiated to a larger fluence. Moreover, it means that in the samples irradiated to $\Phi = 5 \times 10^{17} \text{ e}^- \text{ cm}^{-2}$ or more the negative ions have a large influence on the average lifetime even at 300 K.

The concentration of the vacancies and negative ions can be quantitatively estimated by calculating the positron trapping rates κ_v and κ_{st} at the vacancies and ions using Eqs. (4) and (6). In the data of the GaAs(Te) sample irradiated to $\Phi = 1 \times 10^{17} \text{ e}^- \text{ cm}^{-2}$ (Fig. 3), the trapping rate at vacancies κ_v varies as a function of the annealing temperature due to the recovery of the Ga vacancies. For example, after annealing at 345 K we obtain the trapping rate of $\kappa_v = 4.1 \text{ ns}^{-1}$ for Ga vacancies at 300 K. This value is larger than that obtained earlier in undoped SI GaAs after similar irradiation and annealing.⁹ At least the same amount of Ga vacancies is thus produced by the irradiations in n -type GaAs as in undoped GaAs, although the level of the average lifetime in the recovery curve (Fig. 2) is much lower in the case of n -type material. This observation implies that the average lifetime in Fig. 2 is more strongly influenced by the presence of negative ions than the similar curve in SI GaAs.

We have analyzed the data of Figs. 3 and 4 by fitting Eqs. (5)–(8) to the experimental average lifetime. The solid lines in Figs. 3 and 4 represent the fit. In this analysis we obtain the positron trapping coefficient μ_{st} and the binding energy $E_{b,st}$ at the negative ions, in addition to the positron trapping rates at the vacancies and at the ions. By analyzing all the curves in Figs. 3 and 4, we consistently obtain the positron binding energy of $E_{b,st} = 50 \pm 10 \text{ meV}$ and the trapping coefficient $\mu_{st} = (5 \pm 2) \times 10^{16} (\text{T/K})^{-0.5} \text{ s}^{-1}$ at the negative ions. These values are about the same as those we obtained previously in semi-insulating GaAs,^{9,17} indicating that the defect acting as the negative ion is the same.

In the analysis of the data the concentrations of the vacancy defects after 250-K annealing are $c_v = (2.5 \pm 0.5) \times 10^{17}$ and $(9 \pm 2) \times 10^{17} \text{ cm}^{-3}$ in the

samples irradiated to the fluences $\Phi=1\times 10^{17}$ and $5\times 10^{17} e^- \text{cm}^{-2}$, respectively (Table II). These concentrations are obtained by fixing the trapping coefficient at vacancies to $\mu_v=1.4\times 10^{15} \text{s}^{-1}$ at 300 K.⁹ When the annealing temperature increases to 450 K the concentration of vacancies decreases about an order of magnitude (Table II). However, the analysis shows that in the sample irradiated to $\Phi=1\times 10^{17} e^- \text{cm}^{-2}$ the concentration of the negative ions c_{st} remains roughly constant at the value of $c_{st}=(1.1\pm 0.3)\times 10^{18} \text{cm}^{-3}$, independently of the recovery of the Ga vacancies at 200–450 K. This trend appears similarly in the analysis of the data in the GaAs(Te) sample irradiated to $\Phi=5\times 10^{17} e^- \text{cm}^{-2}$ (Fig. 4), but the concentration of the negative ions is larger: $c_{st}=(5.0\pm 0.8)\times 10^{18} \text{cm}^{-3}$. Furthermore, in both irradiated samples the concentration of the ions is clearly larger than in the as-grown sample, where we obtained $c_{st}=3\times 10^{17} \text{cm}^{-3}$ (Sec. III).

The concentrations of Ga vacancies and negative ions are presented in Fig. 5 as functions of the electron-irradiation fluence. The concentration of V_{Ga} is taken after 250-K annealing, whereas the concentration of negative ions is independent of temperature up to 450 K. Both the Ga vacancy and the negative ion concentrations depend linearly on the irradiation fluence, which is a clear sign that both defects are introduced in the electron irradiation. The introduction rate of Ga vacancies is 2.0cm^{-1} after annealing at 250 K. Since the Ga vacancies recover at 250–300 K, the introduction rate after 300-K annealing is about an order of magnitude lower, roughly $0.1\text{--}0.2 \text{cm}^{-1}$ (see also Ref. 16).

The introduction rate of the negative ions is very large, about 10cm^{-1} (Fig. 5). This value is even larger than that of about 2cm^{-1} we have previously observed in undoped SI GaAs.⁹ We have attributed the negative ions to Ga antisite defects, as they are the only ion-type defects known to be negative in SI GaAs.^{9,17} Since the Fermi level in compensated *n*-type GaAs is at the midgap as in undoped SI GaAs, we can use the same arguments for the charge states of the defects as earlier,^{8,9} and also attribute

the negative ions detected in irradiated *n*-type GaAs to Ga antisites. This identification is further supported by the experimental evidence that in the detrapping analysis both the positron binding energy and trapping coefficient at the ions are the same in irradiated undoped and Te-doped GaAs.

The total concentration of negative ions is clearly larger in compensated *n*-type GaAs than in semi-insulating material. In Fig. 3 almost 300 K is needed to reach the high-temperature plateau, although a constant average lifetime is already detected at 200 K in SI GaAs after similar irradiation.⁹ Furthermore, there is no plateau at all in the data of Fig. 4, whereas in SI GaAs τ_{av} reaches a plateau at 250 K after irradiation to the fluence of $\Phi=5\times 10^{17} e^- \text{cm}^{-2}$.⁹ This difference is partially due to the negative ions already present in the *n*-type material before the irradiation. As explained in Sec. III, in as-grown *n*-type GaAs negative ions are commonly detected, whereas their concentration in as-grown undoped SI GaAs is normally below the detection limit of the positron spectroscopy. The negative ions already formed during the crystal growth stay as effective positron traps after electron irradiation. In addition, the introduction rate of the ions in the irradiation also seems to be larger by a factor of 2–3 in *n*-type GaAs than in SI GaAs. Hence the total concentration of ions after irradiation is clearly larger in compensated *n*-type GaAs than in SI GaAs.

To summarize, we have observed that negative vacancies and negative ions are formed in the electron irradiation of *n*-type GaAs. We attribute them to Ga vacancies and Ga antisites, respectively. Their annealing properties at 80–300 K are similar in compensated *n*-type GaAs and in undoped SI GaAs, but the introduction rate of the Ga antisites is higher in *n*-type material. The positron trapping at native As vacancies is lost in the irradiation, because their charge state becomes positive due to the compensation of the material from *n* type to semi-insulating.

TABLE II. The concentrations of As and Ga vacancies and Ga antisite defects determined in this work after various electron irradiations and isochronal annealing treatments. The sample material was GaAs ($[\text{Te}]=1\times 10^{17} \text{cm}^{-3}$) in all results presented in the table. The irradiation was performed with 1.5-MeV electrons at 20 K. The symbol + indicates that the As vacancies are not detected because of their positive charge state. The symbol < is used in cases where the concentration of Ga vacancies is at least an order of magnitude lower than the As vacancy concentration and thus below the detection limit of the positron lifetime spectroscopy. The vacancy concentrations are obtained by fixing the positron trapping coefficient at negative vacancies to $1.4\times 10^{15} \text{s}^{-1}$ at 300 K.

Irradiation fluence ($e^- \text{cm}^{-2}$)	Annealing temperature (K)	Concentration of As vacancies (10^{17}cm^{-3})	Concentration of Ga vacancies (10^{17}cm^{-3})	Concentration of Ga antisites (10^{17}cm^{-3})
as-grown	300	1.1 ± 0.2	<	3 ± 1
as-grown	600	1.1 ± 0.2	<	3 ± 1
1×10^{17}	250	+	2.6 ± 0.4	11 ± 5
5×10^{17}	250	+	8.8 ± 0.8	42 ± 9
1×10^{17}	450	+	0.5 ± 0.3	11 ± 3
5×10^{17}	450	+	0.9 ± 0.5	50 ± 8
1×10^{17}	550	2.1 ± 0.2	<	7.0 ± 1.5
5×10^{17}	550	3.2 ± 0.3	<	5.0 ± 1.5

V. ANNEALING OF THE DEFECTS AT 300–600 K

A. Recovery of compensation at 550 K

After 20-K irradiation and annealing at 300 K the *n*-type GaAs is compensated to semi-insulating. The native As vacancies are then not detected by positrons due to their positive charge state, but the lifetime experiments reveal irradiation-induced Ga vacancies. At low temperature, positrons are also trapped at the Rydberg states of negative Ga antisite defects produced by irradiation. After the irradiation fluence $\Phi \geq 5 \times 10^{17} \text{ e}^- \text{ cm}^{-2}$, the Ga antisites have an influence on the average positron lifetime even at room temperature.

Figure 6 shows the positron average lifetime as a function of the annealing temperature in two GaAs([Te] = 10^{17} cm^{-3}) samples, which have been irradiated to fluences of $\Phi = 1 \times 10^{17}$ and $5 \times 10^{17} \text{ e}^- \text{ cm}^{-2}$. The measurement temperature is 300 K. In the sample irradiated to the fluence $\Phi = 1 \times 10^{17} \text{ e}^- \text{ cm}^{-2}$ the average lifetime decreases from about 242 to 233 ps in annealings at 350–500 K. After irradiation to the higher fluence of $\Phi = 5 \times 10^{17} \text{ e}^- \text{ cm}^{-2}$ the average lifetime is almost constant at annealing temperatures below 500 K, and its value is less than in the $\Phi = 1 \times 10^{17} \text{ e}^- \text{ cm}^{-2}$ -irradiated sample.

As explained in Sec. IV, the vacancy defects detected after irradiation of *n*-type GaAs are the Ga vacancies.

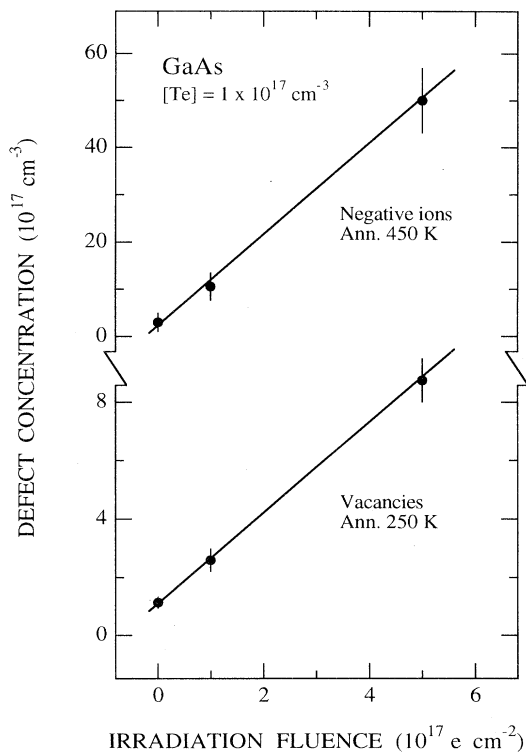


FIG. 5. The concentration of vacancies and negative ions in electron-irradiated Te-doped GaAs as a function of the irradiation fluence. The vacancy concentration is shown after annealing at 250 K, and the ion concentration after annealing at 450 K.

These defects anneal mostly at 200–300 K, but the recovery also continues above room temperature. The decrease of the average lifetime at 300–500 K in the $\Phi = 1 \times 10^{17} \text{ e}^- \text{ cm}^{-2}$ -irradiated GaAs(Te) sample is exactly the same as that we observed previously for Ga vacancies in undoped SI GaAs.⁹ This recovery is not seen well in the $\Phi = 5 \times 10^{17} \text{ e}^- \text{ cm}^{-2}$ -irradiated sample, since positron trapping at negative ions masks the signal from the vacancies by decreasing the average lifetime (see Sec. IV). The remains of the annealing of the Ga vacancies is thus observed in Fig. 6 up to 500 K. Notice that no signs of native As vacancies are detected after annealing at 500 K, but the average lifetime is low, about 233 ps, compared to the value of 238 ps obtained in the as-grown GaAs([Te] = 10^{17} cm^{-3}) at 300 K. This indicates that after annealing at 500 K the Fermi level is still well below the 0/+ ionization level of the native As vacancies, and that the sample is heavily compensated. This conclusion is consistent with the results of electrical measurements, which show no main recovery stages in the resistivity between 300 and 500 K.¹

At annealing temperatures of 500–550 K the positron average lifetime increases steeply. The effect is large since the average lifetime in both samples in Fig. 6 increases by about 10 ps within an annealing temperature range of 20 K. Furthermore, after annealing the sample

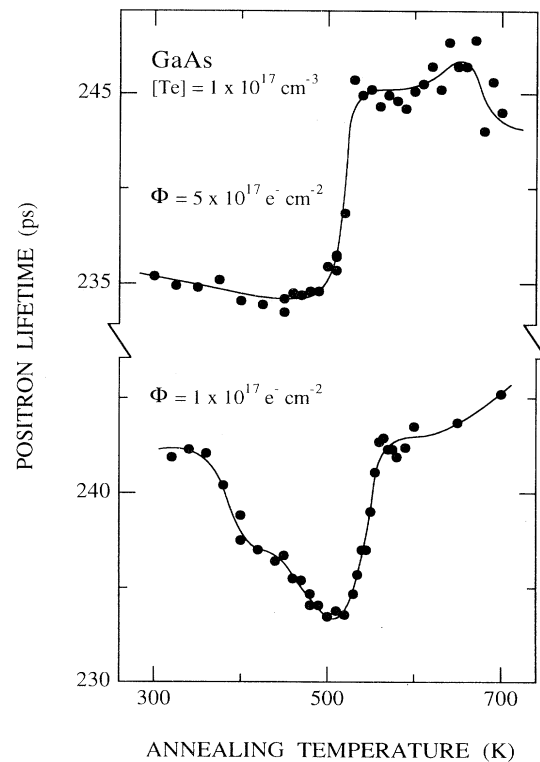


FIG. 6. Positron average lifetime as a function of the isochronal annealing temperature in electron-irradiated Te-doped GaAs. The measurement temperature is 300 K. The figure shows the data after irradiation to fluences of $\Phi = 1 \times 10^{17} \text{ cm}^{-2}$ and $\Phi = 5 \times 10^{17} \text{ cm}^{-2}$. The carrier concentration of the sample was $1 \times 10^{17} \text{ cm}^{-3}$ at 300 K before irradiation.

at 520–550 K the level of the average lifetime seems to be correlated to the irradiation fluence: $\tau_{av}=238$ ps in the as-grown reference sample, $\tau_{av}=242$ ps after $\Phi=1 \times 10^{17} e^- cm^{-2}$ irradiation and $\tau_{av}=245$ ps after the fluence of $\Phi=5 \times 10^{17} e^- cm^{-2}$.

The increase of average lifetime indicates that more vacancy defects become visible to positrons after annealing at 520 K. This conclusion is especially straightforward in the $\Phi=1 \times 10^{17} e^- cm^{-2}$ -irradiated sample, where the negative ions do not trap positrons at 300 K, and the vacancy-type defects are thus the only ones that contribute to the average lifetime (Fig. 3). However, the detection of more vacancies in the positron experiments does not necessarily mean that the vacancies are generated in the annealing process. Rather, the effect may be due simply to movement of the Fermi level toward the conduction band, which changes the charge states of some vacancy defects in such a way that the vacancies are converted to effective positron traps (i.e., from positive to neutral or negative). In fact, we have performed a Hall experiment in one of the irradiated samples after annealing at 600 K. The results show that the *n*-type conductivity has recovered during the annealing, although the sample was semi-insulating after 300- and 500-K annealings, as explained above.

The irradiation-induced compensation of the GaAs samples is thus lost at the same time as more vacancies appear in the positron lifetime experiment. As explained in Sec. III, the native As vacancies are the dominant positron traps in as-grown *n*-type GaAs. However, after irradiation the As vacancies are not observed because they have become positively charged due to the compensation. The present results indicate that the compensation is lost, and that the Fermi level moves back to the conduction band after annealing at 520 K. In this process the native As vacancies become neutral or negative and behave again as efficient positron traps. Hence at least the charge-state transitions $+ \rightarrow 0$ and $0 \rightarrow -$ of the native As vacancies contribute to the increase of the average lifetime at 520 K. In fact, the correlation between the average lifetime and the irradiation fluence indicates that more vacancies are detected after electron irradiation and annealing at 520 K than in the as-grown material. These vacancies are introduced in the irradiation and we shall return to their properties in Sec. V B.

To investigate the amount of negative Ga antisites present after the 520-K stage, we measured the positron lifetime as a function of the measurement temperature in the irradiated and annealed GaAs. Figure 7 presents the data from the GaAs([Te] $=10^{17} cm^{-3}$) samples, which were also used in the annealing study of Fig. 6. The curves from both irradiated samples have been measured after the increase of τ_{av} in the annealing curve, and in Fig. 7 they are also compared to the average lifetime in the as-grown GaAs(Te).

It is seen that the temperature dependence of τ_{av} is qualitatively very similar in both irradiated and as-grown samples, but the absolute levels of the average lifetimes are slightly different. The temperature dependence in the as-grown sample was already explained in Sec. III. When temperature is lowered at $T < 200$ K the average lifetime

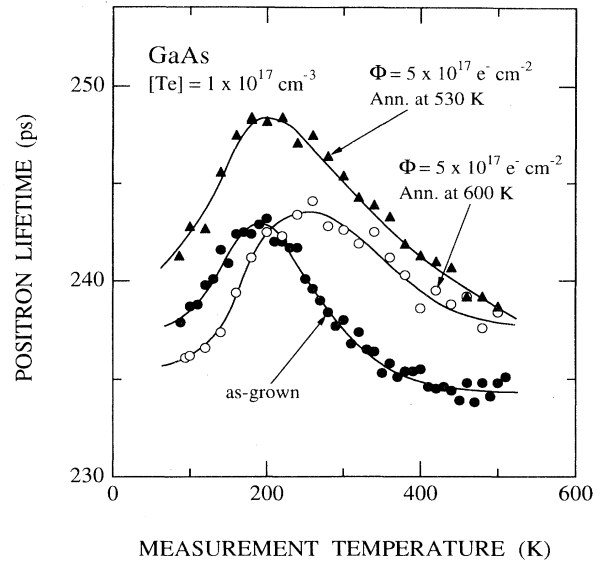


FIG. 7. Positron average lifetime as a function of the measurement temperature in as-grown and electron-irradiated Te-doped GaAs. The carrier concentration of the sample was $1 \times 10^{17} cm^{-3}$ at 300 K before irradiation. The electron-irradiation fluences and the annealing temperatures of the samples are indicated in the figure.

decreases due to positron trapping at negative ions, identified as Ga antisites. The data in Fig. 6 indicate that a temperature of about 200 K is enough to remove the influence of the negative ions both in as-grown and irradiated samples, since the increase of τ_{av} levels off at this temperature in all three curves of Fig. 6. As explained in Sec. IV and in more detail in our earlier work,⁹ this behavior indicates that the concentration of the negative ions is about the same in all the three GaAs(Te) samples. However, below the annealing stage at 520 K the concentration of negative ions (Ga antisites) depends linearly on the irradiation fluence (Fig. 5). Hence we conclude that the irradiation-induced negative ions recover at the 520-K stage, and only the ions present already in the as-grown material remain in the sample after the annealing at 520 K.

This conclusion is also reached after quantitative analysis of the data. Using Eqs. (5)–(8), we can model the temperature dependence of the average lifetime and obtain the concentrations of the vacancies and of the negative ions as fitting parameters. The concentration of the negative ions is $c_{st}=3 \times 10^{17} cm^{-3}$ in as-grown GaAs(Te) (Sec. III), and in the two irradiated samples we obtain $c_{st}=1.1 \times 10^{18} cm^{-3}$ ($\Phi=1 \times 10^{17} e^- cm^{-2}$) and $c_{st}=5 \times 10^{18} cm^{-3}$ ($\Phi=5 \times 10^{17} e^- cm^{-2}$) after annealing at 300 K. The concentration of the negative ions depends on the irradiation fluence (Fig. 5). Between 300 and 450 K there is no change in the concentration of the negative ions, as found earlier⁹ or by analyzing the data of Fig. 3 (Table II). However, after annealing the irradiated samples at 520–600 K (Fig. 7), we obtain the concentrations $c_{st}=(7.0 \pm 1.5) \times 10^{17} cm^{-3}$ ($\Phi=1 \times 10^{17}$

$e^- \text{cm}^{-2}$) and $c_{\text{st}} = (5.0 \pm 1.5) \times 10^{17} \text{ cm}^{-3}$ ($\Phi = 5 \times 10^{17} e^- \text{cm}^{-2}$) at the negative ions. These values are practically the same as in the as-grown sample (Table II). Furthermore, they do not depend on the irradiation fluence, as shown in the upper panel of Fig. 8. The quantitative analysis thus confirms that the negative ions formed during the electron irradiation recover after annealing at 520 K.

The removal of the compensation at 520 K means that the irradiation-induced defect responsible for the compensation disappears. The present positron experiments indicate that the negative ions introduced by the irradiation recover at 520 K. The negative ions are identified as Ga antisite defects. Being negatively charged, possibly in $2-$ state,^{26–28} the Ga antisites are acceptors and thus able to compensate the n -type material. The compensation due to them can be very efficient, since the introduced rate of Ga_{As} is large, about 10 cm^{-1} , even after 300-K annealing. We thus conclude that Ga antisite plays a major role in the conversion of n -type GaAs to semi-insulating GaAs in the electron irradiation. The compensation is lost and the n -type conductivity recovered when the Ga antisite defects anneal at 520 K.

B. Properties of irradiation-induced As vacancies

The data in Figs. 6 and 7 indicate that the average lifetime in the irradiated samples after annealing at 520 K is higher than in the as-grown material. The increase of τ_{av}

at 500–520 K in Fig. 6 is at least partially due to the native As vacancies, which convert from positive to neutral or negative when the compensation of the sample is removed. After annealing at these temperatures the negative ions make no contribution to the average lifetime at 300 K (Sec. V A). The high values of the average lifetime thus suggest that more vacancy-type defects are observed in the irradiated and annealed samples than in the as-grown material.

As explained in Sec. III, the decrease of the positron average lifetime in the as-grown GaAs(Te) at 200–550 K is due to two ionizations of the native As vacancies, first from negative to neutral charge state and finally to a positive charge state. In the ionization $V_{\text{As}}^- \rightarrow V_{\text{As}}^0$ the positron lifetime at the vacancy τ_2 increases from 257 to 295 ps due to lattice relaxation (see Fig. 1). The data in Fig. 7 indicate that the corresponding decrease in the positron average lifetime is also seen in the irradiated GaAs(Te) samples, although the level of τ_{av} is clearly higher. This behavior suggests that the vacancies in the irradiated samples exhibit similar ionizations as in the as-grown material.

The decomposition of the lifetime spectra in the $\Phi = 5 \times 10^{17} e^- \text{cm}^{-2}$ -irradiated GaAs(Te) after annealing at 530 K is shown in Fig. 9. The lifetime component τ_2 increases smoothly from about 260 ps at 100 K to 280 ps at 500 K. This transition is exactly the same as that seen in the as-grown material (Fig. 1), thus confirming that the vacancies in the irradiated and annealed samples

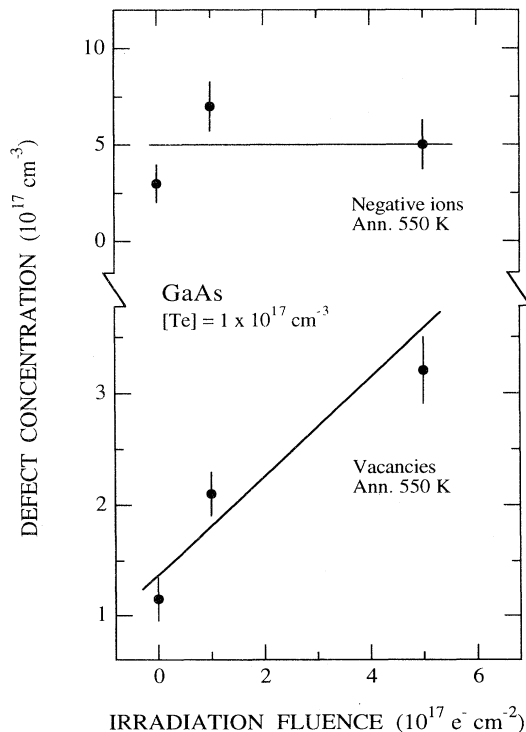


FIG. 8. The concentration of the vacancies and negative ions in electron-irradiated Te-doped GaAs as a function of the irradiation fluence. Both the vacancy and the ion concentrations are shown after annealing at 550 K.

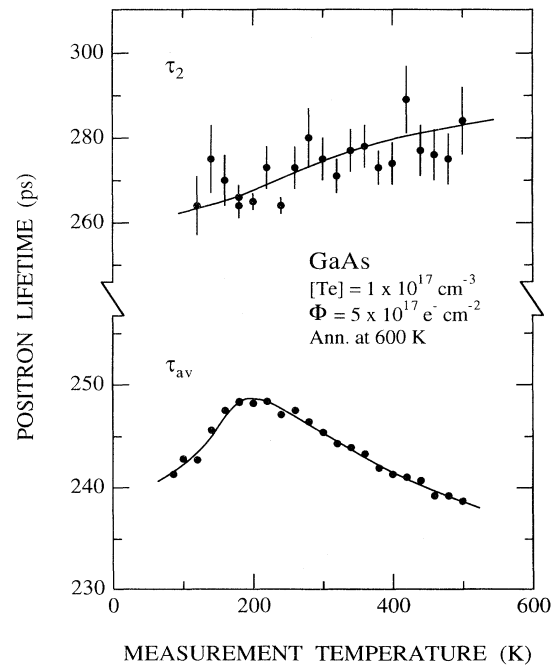


FIG. 9. Positron average lifetime and the second lifetime component as a function of measurement temperature in electron-irradiated Te-doped GaAs. The sample has been electron irradiated to a fluence of $\Phi = 5 \times 10^{17} \text{ cm}^{-2}$ and subsequently annealed at 600 K. The carrier concentration of the sample was $1 \times 10^{17} \text{ cm}^{-3}$ at 300 K before irradiation.

exhibit the ionization of the As vacancy from negative to neutral charge states. A similar decomposition is also obtained from the GaAs(Te) sample irradiated to $\Phi = 1 \times 10^{17} \text{ e}^- \text{ cm}^{-2}$ and annealed at 600 K. Since the positron lifetime component τ_2 is the same in the irradiated and in as-grown GaAs(Te) at all temperatures, the average lifetime curves in Fig. 7 can only be explained by different vacancy concentrations in the irradiated and as-grown material.

This analysis gives positive evidence that more vacancy defects are observed in the irradiated and 520-K annealed samples than in the as-grown *n*-type GaAs. The concentration of the vacancies is proportional to the irradiation fluence (Fig. 7), which shows that the detected vacancies are introduced in the electron irradiation. Furthermore, the irradiation-induced vacancies exhibit the same lifetime transition from $\tau_2 = 257$ to 295 ps as the native As vacancies, since the lifetime component τ_2 increases in almost exactly the same way as a function of temperature in the as-grown (Fig. 1) and irradiated (Fig. 9) GaAs(Te), although the vacancy concentrations are different.

The irradiation-induced Ga vacancies recover mostly at 200–300 K, and minor annealing effects are detected up to 500 K (Fig. 6). However, the difference between the average lifetimes in Fig. 7 is much too large to be caused by the Ga vacancies remaining in the irradiated *n*-type GaAs after 520-K annealing. Rather, the irradiation-induced vacancies detected after 520-K annealing do not act as positron traps as long as the irradiated sample stays compensated, i.e., at annealing temperatures below 500 K. Only when the compensation is lost in the annealing at 520 K, and the Fermi level moves toward the conduction band, do the vacancies become attractive to positrons. This means that the irradiation-induced vacancies must have their $+/0$ ionization level above midgap. Furthermore, the data in Fig. 9 suggest that the irradiation-induced vacancies exhibit the same Fermi-level-controlled lifetime transitions as observed for the As vacancy in the as-grown material in this work (Sec. III) or earlier.^{12,18} The lifetime values of 257 and 295 ps are in good agreement with the theoretical positron lifetime calculations for the As vacancy.^{19,20} Based on these arguments, we identify the defects as As vacancies. After annealing at 550 K the irradiated GaAs(Te) samples thus contain both native As vacancies and those created in the electron irradiation. The irradiation-induced V_{As} are responsible for the fluence dependence of the positron average lifetime seen in Fig. 7.

The amount of As vacancies introduced in the electron irradiation can be quantitatively estimated using the positron trapping model. By modeling the temperature dependence of the average lifetime with Eqs. (5)–(8), we obtain information about the concentrations of both vacancies and negative ions. In this analysis we describe the ionizations of the As vacancies with the Fermi functions similarly as explained in Sec. III. Since the exact position of the Fermi level in the irradiated samples is not known after annealing at 550–600 K, we use the temperature dependence of the Fermi level determined in the as-grown samples. This choice can be justified, since the original electrical conductivity of the samples recovers in

the annealing at 520 K, as explained above in Sec. V A. In any case, we have found by analyzing the data that the concentrations of vacancies and negative ions are insensitive to the uncertainties in the position of the Fermi level. We further use the positron trapping coefficient $\mu_v = 1.4 \times 10^{15} \text{ s}^{-1}$ at 300 K to determine the vacancy concentration.

The concentration of the As vacancies is shown as a function of the irradiation fluence in the lower panel of Fig. 8 and in Table II. Notice that the data after electron irradiation are measured after annealing at 550 K, and the results from the as-grown sample appear at the fluence $\Phi = 0$ in Fig. 8. The concentration of the As vacancies depends linearly on the fluence, and we obtain the introduction rate $\Sigma(V_{\text{As}}) = 0.5 \text{ cm}^{-1}$. This introduction rate is small, but in our measurements we are able to detect the As vacancies only after annealing at 520 K. If there are recovery stages related to V_{As} at lower temperatures they are missed in the positron experiments due to the positive charge state of V_{As} .

In conclusion, after the removal of the compensation of irradiated *n*-type GaAs we are able to detect the native As vacancies already found in the as-grown GaAs. In addition, we observe As vacancies formed during the electron irradiation. The introduction rate of these vacancies is about 0.5 cm^{-1} , measured after annealing at 550 K. The irradiation-induced As vacancies have the same ionization levels in the gap as the native ones.

VI. RECOVERY OF IRRADIATION-INDUCED DEFECTS AT 600–700 K

After annealing at 520 K the irradiation-induced As vacancies change their charge state from positive to negative, and they can thus be detected in positron lifetime experiments. By annealing the samples at higher temperatures it is then possible to study the recovery of the As vacancies. The annealing stages below 800 K can be directly associated with defects introduced in the electron irradiation, because the native As vacancies detected in as-grown GaAs are stable up to this temperature.¹²

The positron average lifetime is shown in Fig. 6 as a function of the annealing temperature in the irradiated GaAs([Te] = 10^{17} cm^{-3}). The behavior of τ_{av} at annealing temperatures of 600–700 K is complicated: in the $\Phi = 5 \times 10^{17} \text{ e}^- \text{ cm}^{-2}$ -irradiated sample τ_{av} stays constant or decreases, but in the $\Phi = 1 \times 10^{17} \text{ e}^- \text{ cm}^{-2}$ -irradiated sample τ_{av} increases as a function of annealing temperature. As explained in Sec. V, in this type of sample the positron average lifetime measured at 300 K may depend strongly on the position of the Fermi level, because the ionization of the As vacancy from negative to neutral takes place around this temperature. The concentration of shallow Te donors in the samples studied in Fig. 6 is very close to the concentration of the As vacancies: $[\text{Te}] \approx [V_{\text{As}}] \approx 10^{17} \text{ cm}^{-3}$. Because the negative As vacancies compensate the Te donors at least partially, the recovery of V_{As} has an influence on the position of the Fermi level. As a consequence, the occupation of the negative and neutral states of the *native* As vacancies may change when the *irradiation-induced* As vacancies

recover. These processes may result in a complicated response in the measured average positron lifetime, as possibly seen in the data of Fig. 6. However, this type of problem may be overcome by studying heavily doped samples, where the concentration of donor impurities is much larger than that of the As vacancies, i.e., $[Te] \approx 10^{18} \text{ cm}^{-3} \gg [V_{As}]$. In that case the recovery of V_{As} has only a minor effect on the position of the Fermi level.

Figure 10 shows the isochronal annealing of the positron average lifetime in $\Phi = 5 \times 10^{17} \text{ e}^- \text{ cm}^{-2}$ -irradiated GaAs ($[Si] = 2.3 \times 10^{18} \text{ cm}^{-3}$), and in $\Phi = 1 \times 10^{18} \text{ e}^- \text{ cm}^{-2}$ -irradiated GaAs ($[Te] = 5 \times 10^{18} \text{ cm}^{-3}$). The data indicate that the large increase of τ_{av} associated with the recovery of the Ga antisites (Sec. V A) takes place at slightly lower temperatures of 450–500 K than observed in Fig. 5 for the samples with the doping level of $[Te] = 10^{17} \text{ cm}^{-3}$. This shift is consistent with the idea that the stage is connected to the removal of the compensation created by the irradiation: if the donor concentration is larger, the compensation is less efficient, and a smaller recovery fraction of acceptors is needed to shift the Fermi level back to the conduction band.

The irradiation-induced As vacancies are well seen in Fig. 10, since the average lifetime after 500-K annealing depends strongly on the irradiation fluence. The second lifetime component τ_2 at 300 K is about 260 ps after all heat treatments at $T > 500 \text{ K}$, indicating that all As vacancies stay in the negative charge state independently of the possible recoveries of these or other irradiation-induced defects. As expected, the position of the Fermi level in the heavily doped samples is thus controlled completely by the shallow impurities at the annealing temperatures $T > 500 \text{ K}$.

The average lifetime in Fig. 10 decreases clearly at

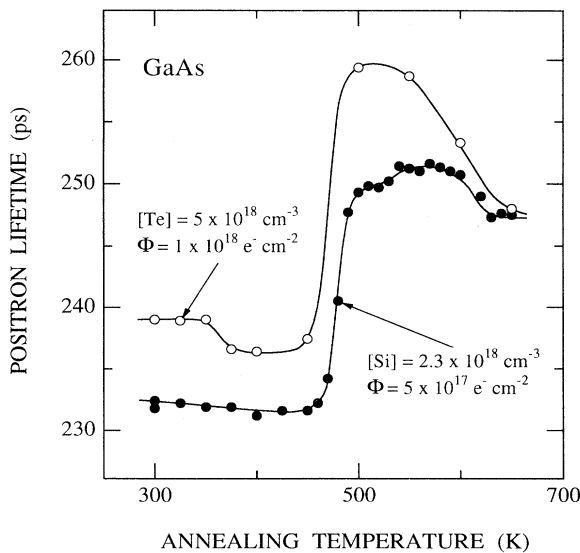


FIG. 10. Positron average lifetime as a function of the isochronal annealing temperature in electron-irradiated *n*-type GaAs. The measurement temperature is 300 K. The donor atom, the carrier concentration of the samples at 300 K before irradiation, and the irradiation fluence are indicated in the figure.

about 550–650 K. Since the second lifetime component τ_2 remains constant over this temperature range, the decrease of τ_{av} is associated with the recovery of vacancy defects. As explained above, irradiation-induced As vacancies are detected after annealing the sample at 500 K, and Ga vacancies have been recovered earlier at 200–300 K. Furthermore, the native As vacancies are stable at least up to 800 K. We thus associate the stage detected at 550–650 K in Fig. 10 with the recovery of the As vacancies created in the electron irradiation. After annealing at these temperatures the positron average lifetime does not depend on the irradiation fluence, suggesting that the recovery after electron irradiation is completed.

VII. IDENTIFICATION OF THE ANNEALING STAGES IN ELECTRON-IRRADIATED GALLIUM ARSENIDE

The present and earlier positron experiments^{8,9} have revealed the following annealing stages of the irradiation-induced defects in GaAs: (i) The Ga vacancies recover at 200–300 K. (ii) The Ga antisite defects anneal at 500–550 K. (iii) The As vacancies recover at 550–650 K. In this section we shall correlate these findings with the existing electrical, optical, and electron paramagnetic resonance (EPR) results on the electron irradiation of GaAs.

The electrical measurements by Thommen revealed three annealing stages at 235, 280, and 520 K.⁴ The temperatures of these recovery stages correlate well with the observations by positron annihilation, since the largest effects in the positron lifetime are indeed seen at 200–300 and 500–550 K. More recently, Siyanbola and Palmer have determined the positions of the energy levels of the defects annealing at 200–300 K.²⁹ Using electrical techniques, they located three levels at 0.16, 0.25, and 0.42 eV above the valence band. Since the positron experiments indicate that the Ga vacancy recovers at 200–300 K, the levels determined by Siyanbola and Palmer can be attributed to the ionization levels of the Ga vacancy. The annealing of the Ga vacancy at 200–300 K has been also observed by EPR and x-ray techniques.^{30–32} Jia *et al.* determined by EPR the introduction rate of 0.03 cm^{-1} for the Ga vacancy after 1-MeV electron irradiation and 300-K annealing,³⁰ which is in reasonable agreement with our value of 0.10 cm^{-1} after 1.5-MeV irradiation. The defect concentrations found using the positron lifetime spectroscopy are thus consistent with those detected in the EPR experiments.

The formation of Ga and As antisite defects in the electron irradiation of GaAs has been studied recently by molecular-dynamics simulations.³ The results indicate that stable antisites can be formed directly during focused collision cascades. The introduction rates obtained from the simulations are of the same order of magnitude as those estimated for Ga_{As} and As_{Ga} in the present work or earlier.^{9,17}

Previous experimental information about the production and annealing of the Ga antisite defects is very limited. However, Jia *et al.* recently observed Ga_{As} by EPR techniques.^{33,34} According to their results the Ga antisite

anneals at 500 K, which fits the observations of this work by positron annihilation very well. The recovery stage at 500 K is also equivalent to that of the hole traps $H0$ and $H1$, which are located at 0.06 and 0.29 eV above the valence band in deep-level transient spectroscopy (DLTS) measurements.^{2,35} The comparison of their annealing temperature with the results of the present work suggests that these levels can be related to the Ga antisite defect.

Heat treatment at 500 K results in the annealing of the irradiation-induced electron traps $E1$ – $E5$ in DLTS measurements.^{2,36,37} These defects have been related to As vacancies which are isolated or bound to an interstitial atom.^{2,38,39} The ionization levels of traps $E1$ and $E2$ are 45 and 140 meV below the conduction band. These values fit well with those determined for the As vacancy in the present positron annihilation experiments. In this work we observed the annealing stage of the As vacancies at slightly higher temperatures of 550–600 K than the recovery of $E1$ and $E2$ in DLTS. However, in the positron experiments the As vacancies are *detected* only after annealing at about 550 K, when the compensation of the sample is removed and the Fermi level moves toward the conduction band (Sec. V). If the recovery starts earlier than 550 K, it is not observed in the positron measurements. In fact, the same reason could explain the differences in the introduction rates: 0.5 cm^{-1} was estimated for V_{As} in this work, whereas 1.5 cm^{-1} has been determined for traps $E1$ and $E2$ in DLTS.² Our value of 0.5 cm^{-1} is again obtained after annealing the sample at 550 K, which may be above the main recovery stage of the V_{As} . The data in Fig. 10 even suggest that recovery of V_{As} has already started at 500 K, and that the introduction rate could be higher than 0.5 cm^{-1} . We thus conclude that the results of this work are in agreement with the association of traps $E1$ and $E2$ to the As vacancy.

Recovery of the irradiation-induced As vacancies has also been studied by EPR measurements.³⁵ The results show that only part of the As vacancies anneal at 500 K and the stage continues up to about 700 K. These observations are in good agreement with the results of this work on the recovery of the As vacancies. Annealing stages at 200–300 and 500–600 K have also been detected in infrared-absorption measurements.⁴⁰ After electron irradiation the absorption spectrum of GaAs consists of a featureless background at $h\nu \leq 1.2 \text{ eV}$ and a strong increase in the absorption coefficient at $h\nu \geq 1.2 \text{ eV}$. In addition, two broad peaks are commonly observed at 0.8 and 0.98 eV. The background absorption at $h\nu \leq 1.2 \text{ eV}$ recovers mainly at 200–300 K, which correlates well with the annealing of the Ga vacancy in the positron experiments. The strong absorption at $h\nu \geq 1.2 \text{ eV}$ and the peaks at 0.8 and 0.98 eV recover at higher temperatures of 500–600 K, which are close to those observed for the annealing of the Ga antisite and As vacancy in this work. The present positron results may thus be helpful in identifying which parts of the absorption spectrum are due to Ga vacancies, and Ga antisite defects.

In conclusion, the recovery stages of point defects found in this work can be related to various effects observed in electrical, optical, and EPR experiments. However, the recovery processes may also involve defects which are inaccessible by positron techniques due to their structure or charge state. The firm identification of the annealing mechanisms thus requires a systematic combination of the information obtained by several experimental probes.

VIII. CONCLUSIONS

In this work we have studied the introduction and annealing of defects in n -type Te and Si-doped GaAs irradiated by 1.5-MeV electrons. The 20-K irradiation was followed by isochronal annealings from 100 to 700 K. The characterization of the as-grown n -type GaAs by positron experiments reveals native As vacancies in good agreement with the results of our earlier works.^{18,12} After electrical compensation of the samples by the electron irradiation, two types of acceptor defects are found in the positron experiments: the Ga vacancies and the Ga antisite defects. The Ga vacancies recover mainly at 200–300 K, whereas the Ga antisites remain stable at this annealing stage. The production of V_{Ga} and Ga_{As} in the electron irradiation is found to be similar in n -type GaAs to what was observed earlier in undoped SI GaAs.⁹

After annealing at 520 K the compensation due to the irradiation is removed, and the n -type conductivity of Te- and Si-doped GaAs recovers. The present positron experiments show that this stage is related to the annealing of the Ga antisite defects. The antisites are negatively charged and their introduction rate is large, about 10 cm^{-1} in 1.5-MeV electron irradiation followed by annealing at 300 K. We thus conclude that the negative Ga antisites are very effective acceptors, and play a crucial role in the compensation of the n -type GaAs in the electron irradiation.

After annealing at 520 K, positron experiments reveal As vacancies which convert from a positive charge state to neutral or negative during the removal of the compensation at 520 K. Some of the As vacancies are those already formed during the crystal growth, but some of them are introduced during the electron irradiation. Both populations of V_{As} have similar ionization levels in the gap, and the $0/-$ level is located at about 30 meV below the conduction band. Irradiation-induced As vacancies recover at 550–650 K, whereas the native ones are stable up to 800 K. The introduction rate of the As vacancies determined after annealing at 550 K is 0.5 cm^{-1} . This low value may indicate that the recovery of V_{As} has already started below 550 K.

ACKNOWLEDGMENTS

We are grateful to F. Pierre and S. Simula for their help in the experiments and in the data analysis.

- ¹D. V. Lang, in *Radiation Effects in Semiconductors*, edited by N. B. Orli and J. W. Corbett, IOP Conf. Proc. No. 31 (Institute of Physics and Physical Society, London, 1977), p. 70.
- ²D. Pons and J. C. Bourgoin, *J. Phys. C* **18**, 3839 (1985).
- ³T. Mattila and R. M. Nieminen, *Phys. Rev. Lett.* **74**, 2721 (1995).
- ⁴K. Thommen, *Radiat. Eff.* **2**, 201 (1970).
- ⁵*Positrons in Solids*, edited by P. Hautojärvi, Topics in Current Physics Vol. 12 (Springer-Verlag, Heidelberg, 1979).
- ⁶*Positron Solid State Physics*, edited by W. Brandt and A. Dupasquier (North-Holland, Amsterdam, 1983).
- ⁷K. Saarinen, P. Hautojärvi, A. Vehanen, R. Krause, and G. Dlubek, *Phys. Rev. B* **39**, 5287 (1989).
- ⁸C. Corbel, F. Pierre, P. Hautojärvi, K. Saarinen, and P. Moser, *Phys. Rev. B* **41**, 10 632 (1990).
- ⁹C. Corbel, F. Pierre, K. Saarinen, P. Hautojärvi, and P. Moser, *Phys. Rev. B* **45**, 3386 (1992).
- ¹⁰M. Stucky, C. Corbel, B. Geffroy, P. Moser, and P. Hautojärvi, in *Defects in Semiconductors*, edited by H. J. von Bardeleben, Materials Science Forum Vols. 10–12 (Trans Tech, Aedermannsdorf, 1986), p. 265.
- ¹¹R. Würshum, W. Bauer, K. Maier, A. Seeger, and H.-E. Schaefer, *J. Phys. Condens. Matter* **1**, SA33 (1989).
- ¹²C. Corbel, M. Stucky, P. Hautojärvi, K. Saarinen, and P. Moser, *Phys. Rev. B* **38**, 8192 (1988).
- ¹³M. J. Puska, C. Corbel, and R. M. Nieminen, *Phys. Rev. B* **41**, 9980 (1990).
- ¹⁴J. Mäkinen, C. Corbel, P. Hautojärvi, P. Moser, and F. Pierre, *Phys. Rev. B* **39**, 10 162 (1989).
- ¹⁵J. Mäkinen, P. Hautojärvi, and C. Corbel, *J. Phys. Condens. Matter* **3**, 7217 (1991).
- ¹⁶C. LeBerre, C. Corbel, K. Saarinen, S. Kuisma, P. Hautojärvi, and R. Fornari, *Phys. Rev. B* **52**, 8112 (1995).
- ¹⁷K. Saarinen, S. Kuisma, J. Mäkinen, P. Hautojärvi, M. Törnqvist, and C. Corbel, *Phys. Rev. B* **51**, 14 152 (1995).
- ¹⁸K. Saarinen, P. Hautojärvi, P. Lanki, and C. Corbel, *Phys. Rev. B* **44**, 10 585 (1991).
- ¹⁹M. J. Puska and R. M. Nieminen, *Rev. Mod. Phys.* **66**, 841 (1994).
- ²⁰K. Laasonen, M. Alatalo, M. J. Puska, and R. M. Nieminen, *J. Phys. Condens. Matter* **3**, 7217 (1991).
- ²¹B. Barbiellini, M. J. Puska, T. Torsti, and R. M. Nieminen, *Phys. Rev. B* **51**, 7341 (1995).
- ²²A. A. Rezaadeh and D. W. Palmer, *J. Phys. C* **18**, 43 (1985).
- ²³D. C. Look and J. R. Sizelove, *J. Appl. Phys.* **62**, 3660 (1987).
- ²⁴D. C. Look, *Solid State Commun.* **64**, 805 (1987).
- ²⁵P. Hautojärvi, P. Moser, M. Stucky, C. Corbel, and F. Plazaola, *Appl. Phys. Lett.* **48**, 809 (1986).
- ²⁶J. C. Bourgoin, H. J. von Bardeleben, and D. Stievenard, *J. Appl. Phys.* **64**, R65 (1988), and references therein.
- ²⁷G. A. Baraff and M. Schlüter, *Phys. Rev. Lett.* **55**, 1327 (1985).
- ²⁸M. J. Puska, *J. Phys. Condens. Matter* **1**, 7347 (1989).
- ²⁹W. O. Siyanbola and D. W. Palmer, *Phys. Rev. Lett.* **66**, 56 (1991).
- ³⁰Y. Q. Jia, H. J. von Bardeleben, D. Stievenard, and C. Delerue, *Phys. Rev. B* **45**, 1645 (1992).
- ³¹K. Krambrock and J.-M. Spaeth, *Solid State Commun.* **93**, 285 (1995).
- ³²A. Pillukat and P. Ehrhart, in *Defects in Semiconductors*, edited by G. Davies, G. G. DeLeo, and M. Stavola, Materials Science Forum Vols. 83–87 (Trans. Tech, Aedermannsdorf, 1992), p. 947.
- ³³Y. Q. Jia, H. J. von Bardeleben, D. Stievenard, and C. Delerue, in *Defects in Semiconductors* (Ref. 32), p. 965.
- ³⁴Y. Q. Jia, These de Doctorat de l'Universite Paris, 1992 (unpublished).
- ³⁵D. Stievenard, X. Boddaert, J. C. Bourgoin, and H. J. von Bardeleben, *Phys. Rev. B* **41**, 5271 (1990).
- ³⁶D. V. Lang, L. C. Kimerling, and S. Y. Leung, *J. Appl. Phys.* **47**, 3587 (1976).
- ³⁷D. Pons, A. Mircea, and J. Bourgoin, *J. Appl. Phys.* **51**, 4150 (1980).
- ³⁸S. Loualiche, G. Guillot, A. Nouailhat, and J. Bourgoin, *Phys. Rev. B* **26**, 7090 (1982).
- ³⁹S. Loualiche, A. Nouailhat, G. Guillot, and M. Lannoo, *Phys. Rev. B* **30**, 5822 (1984).
- ⁴⁰A. Pillukat and P. Ehrhart, *Phys. Rev. B* **45**, 8815 (1992), and references therein.